ELSEVIER

Advances in Water Resources 25 (2002) 637–649

Advances in Water Resources

www.elsevier.com/locate/advwatres

Analytical solutions to a hillslope-storage kinematic wave equation for subsurface flow

Peter Troch *, Emiel van Loon, Arno Hilberts

Department of Environmental Sciences, Hydrology and Quantitative Water Management Group, Wageningen University, Nieuwe Kanaal 11, 6709 PA Wageningen, Netherlands

Received 25 June 2001; received in revised form 12 February 2002; accepted 19 February 2002

Abstract

Hillslope response has traditionally been studied by means of the hydraulic groundwater theory. Subsurface flow from a one-dimensional hillslope with a sloping aquifer can be described by the Boussinesq equation [Mem. Acad. Sci. Inst. Fr. 23 (1) (1877) 252–260]. Analytical solutions to Boussinesq's equation are very useful to understand the dynamics of subsurface flow processes along a hillslope. In order to extend our understanding of hillslope functioning, however, simple models that nonetheless account for the three-dimensional soil mantle in which the flow processes take place are needed. This three-dimensional soil mantle can be described by its plan shape and by the profile curvatures of terrain and bedrock. This plan shape and profile curvature are dominant topographic controls on flow processes along hillslopes. Fan and Bras [Water Resour. Res. 34 (4) (1998) 921–927] proposed a method to map the three-dimensional soil mantle into a one-dimensional storage capacity function. Continuity and a kinematic form of Darcy's law lead to quasi-linear wave equations for subsurface flow solvable with the method of characteristics. Adopting a power function of the form proposed by Stefano et al. [Water Resour. Res. 36 (2) (2000) 607–617] to describe the bedrock slope, we derive more general solutions to the hillslope-storage kinematic wave equation for subsurface flow, applicable to a wide range of complex hillslopes. Characteristic drainage response functions for nine distinct hillslope types are computed. These nine hillslope types are obtained by combining three plan curvatures (converging, uniform, diverging) with three bedrock profile curvatures (concave, straight, convex). We demonstrate that these nine hillslopes show quite different dynamic behaviour during free drainage and rainfall recharge events.

Keywords: Hillslope hydrology; Subsurface flow; Kinematic wave approximation; Method of characteristics

1. Introduction

A river basin is made up of interconnected hillslopes and the channel network which drains these hillslopes. Both hillslopes and channels transport water to the outlet of the basin. To understand the hydrological processes at the catchment scale is to understand the characteristic response of the hillslopes and the channel network within the catchment. Several researchers have focused attention on modeling the dynamic response of the channel network, by accounting for network geometry [4–6]. The rationale behind this is that both network topology and geomorphology are essential to define the channels' response to a given volume of surface runoff or lateral inflow.

Hillslope response has traditionally been studied by means of hydraulic groundwater theory. Subsurface flow from a one-dimensional hillslope with a sloping aquifer can be described by the Boussinesq equation (1):

$$\frac{\partial h}{\partial t} = \frac{k}{f}\left[\cos i \frac{\partial}{\partial x'}\left(h\frac{\partial h}{\partial x'}\right) + \sin i \frac{\partial h}{\partial x'}\right] \tag{1}$$

where $h(x', t)$ (Fig. 1) is the elevation of the groundwater table measured perpendicular to the underlying impermeable layer which has a slope angle i, k is the hydraulic conductivity, f is drainable porosity, x' is distance from the stream and measured parallel to the impermeable layer, and t is time. We refer to [7,8] for a general discussion of the Boussinesq equation. No general analytical solutions of (1) exist. For horizontal bedrock [9,10] derived exact solutions to (1). When i can be assumed

* Corresponding author. Tel.: +31-317-484397.
E-mail addresses: peter.troch@users.whh.wau.nl (P. Troch), emiel.vanloon@users.whh.wau.nl (E. van Loon), arno.hilberts@users.whh.wau.nl (A. Hilberts).

0309-1708/02/$ - see front matter
PII: S0309-1708(02)00017-9

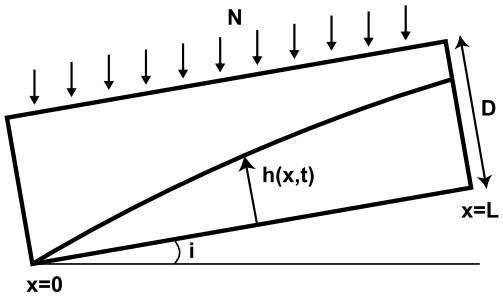

Fig. 1. Definition sketch of the cross-section of a hillslope aquifer.

large, the kinematic wave approach becomes applicable [1,11,12]. In this approximation the second-order diffusive term in (1) disappears, rendering the analytical solution inappropriate for small to intermediate slopes. Examples of kinematic wave modeling of subsurface flow along unit width hillslopes for catchment scale applications can be found in [2,13–15]. Solutions of (1) for small to intermediate slopes have been obtained through linearization [16–19].

These analytical solutions are very useful to understand the dynamics of subsurface flow processes along a hillslope. There is however a need to derive equally simple models and corresponding analyical solutions that account for the three-dimensional soil mantle in which these flow processes take place [20]. This three-dimensional soil mantle can be described by its plan and profile curvature. The plan and profile curvature are the dominant topographic controls on flow processes along hillslopes [21–26]. Essentially, three plan curvatures are encountered in nature: convergent, where slope width increases with distance from the channel; divergent, where slope width decreases with distance; and uniform, where slope width remains more or less constant. Similarly, for profile curvature we can distinguish essentially three types: concave, where slope increases with distance; convex, where slope decreases with distance; and plane, where the slope is more or less constant. Combination of the three plan and the three profile curvatures results in nine distinct hillslope types which may show different dynamic response to storm rainfall. In this paper, we derive the characteristic drainage response functions of these hydrological units under the assumption of kinematic wave subsurface flow, based on a more general analytical solution to the hillslope-storage dynamic equations. The response functions can be extended to include saturation overland flow (including the extent of saturation).

Section 2 describes how the three-dimensional soil mantle can be collapsed into a one-dimensional storage capacity profile. We then formulate the kinematic form of Darcy's equation in terms of soil storage as the dependent variable of interest, and present analytical solutions to these equations based on the method of characteristics. The solution describes the storage and the outflow as functions of time and distance from the divide. We also derive the steady-state solution for a given recharge rate by allowing time to approach infinity.

Section 3 compares the characteristic response functions for nine hillslope types. First, we describe in detail how the different hillslope types used in this study are generated. Then we compute the impulse response functions of subsurface storm flow for these hillslopes. It is found that the nine hillslope types show quite distinct hydrologic behaviour. Next, we compute subsurface storm flow and the corresponding degree of saturation from below during a constant finite duration rainfall recharge event. We illustrate how the proposed model allows the computation of variable source areas induced by topographic controls in a catchment.

Finally, Section 4 summarizes the main results of the paper and discusses some limitations and possible extensions of the approach presented in this paper.

2. Formulation of the hillslope-storage kinematic wave model

2.1. One-dimensional soil moisture storage dynamics

Consider a hillslope with a three-dimensional soil mantle on top of an impermeable layer with given profile curvature (Fig. 2). Flow processes in and over this hillslope will be influenced by its plan and profile curvature, and the hydraulic properties of the porous medium and the surface. The mathematical description of these flow processes results in the formulation of the three-dimensional Richards equation [24,27]. Solving the three-dimensional Richards equation for several hillslopes within a catchment is numerically and computationally a daunting task. Fan and Bras [2] presented

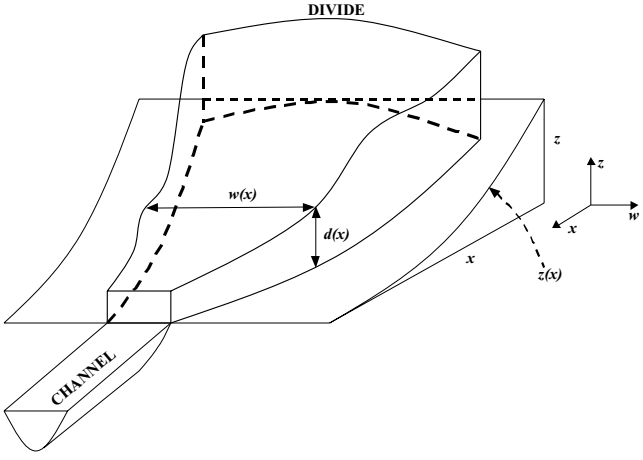

Fig. 2. Three-dimensional view of a convergent hillslope on top of a concave bedrock profile.

a very elegant way to collapse the three-dimensional soil mantle into a one-dimensional profile. They introduced the soil moisture storage capacity function $S_c(x)$, defined as:

$$S_c(x) = w(x)\overline{d}(x)f, \tag{2}$$

where $w(x)$ is the width of the hillslope at flow distance x from the divide (the so-called hillslope width function), $\overline{d}(x)$ is the averaged soil depth at flow distance x, and f is drainable porosity (see also Fig. 2 for a graphical definition of the width and soil depth function). Eq. (2) defines the thickness of the pore space along the hillslope and accounts for both plan curvature, through the width function, and profile curvature, through the soil depth function.

Let us denote with $S(x,t)$ the soil moisture storage at a given flow distance x from the divide and at time t. We can now reformulate the three-dimensional flow problem of Fig. 2 as a one-dimensional flow problem of Fig. 3. The soil moisture storage capacity function, $S_c(x)$, defines the vertical dimension of the hillslope and the propagation of soil moisture storage in space and time, $S(x,t)$, is constrained by the continuity equation and Darcy's law. Along the hillslope the continuity equation reads

$$\frac{\partial S}{\partial t} + \frac{\partial Q}{\partial x} = N(t)w(x), \tag{3}$$

where $N(t)$ is the recharge to the saturated layer. Clearly we have complete saturation whenever $S(x,t) \geqslant S_c(x)$. Let us further assume that the flow rate Q is related to the storage $S(x,t)$ through a kinematic form of Darcy's equation

$$Q = -k\frac{S}{f}\frac{\partial z}{\partial x}, \tag{4}$$

where z is the elevation of the bedrock above a given datum. Combining (4) with the continuity equation for given recharge N and assuming no spatial variability in k and f, one obtains a quasi-linear wave equation in terms of soil moisture storage

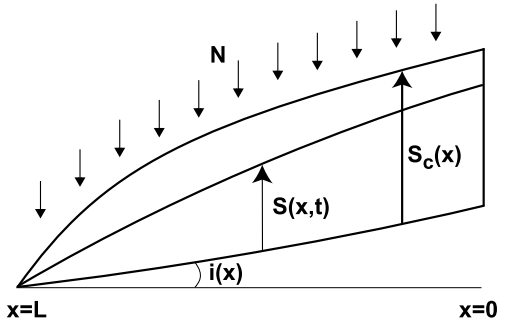

Fig. 3. Definition sketch of the cross-section of a one-dimensional hillslope-storage aquifer on top of a concave bedrock profile.

$$a(x)\frac{\partial S}{\partial x} + \frac{\partial S}{\partial t} = c(x,S), \tag{5}$$

where

$$a(x) = -\frac{kz'(x)}{f},$$

$$c(x,S) = Nw(x) + \frac{kz''(x)}{f}S$$

and $z'(x)$ and $z''(x)$ are first and second derivatives of the bedrock profile curvature function $z(x)$ with respect to x. Fan and Bras [2] proposed a second-order polynomial function of the form

$$z(x) = \alpha + \beta x + \gamma x^2 \tag{6}$$

to describe the hydraulic gradient in the kinematic wave approach. In the following we will use the profile curvature function given by Stefano et al. [3]:

$$z(x) = E + H\left(1 - \frac{x}{L}\right)^n, \tag{7}$$

where H is the elevation difference of the bedrock along the hillslope, L is the corresponding slope length, and the exponent n defines profile curvature. The parameter E defines the reference datum for elevation. Note that when $E = 0$ this equation assumes that the reference datum coincides with the outcrop of the bedrock near the channel. Values of $n > 1$ define concave profiles, $n < 1$ define convex profiles, and for $n = 1$ the profile is linear. Note that for $n = 2$, (7) reduces to (6) with $\alpha = E + H$, $\beta = -2H/L$, and $\gamma = H/L^2$.

2.2. Analytical solutions using (7)

Eq. (5) is a quasi-linear wave equation that can be solved analytically with the method of characteristics. (5) can then be written as a set of ordinary differential equations [2]:

$$\frac{\mathrm{d}x}{\mathrm{d}t} = a(x) = -\frac{kz'}{f}, \tag{8}$$

$$\frac{\mathrm{d}S}{\mathrm{d}x} = \frac{c(x,S)}{a(x)} = -\frac{f}{kz'}N(t)w(x) - \frac{z''}{z'}S \tag{9}$$

(8) describes a family of characteristic curves in the (x,t) plane, and (9) describes how the storage propagates along each curve. Fig. 4 illustrates the method of characteristics in the (x,t) plane. In the context of subsurface flow, it is reasonable to assume the following initial and boundary conditions:

$$S(x,0) = g(x), \quad 0 \leqslant x \leqslant L,$$

$$\frac{\mathrm{d}S(0,t)}{\mathrm{d}x} = 0 \quad \forall t,$$

where $g(x)$ represents the initial soil moisture storage along the hillslope. For subsurface flow and rainfall

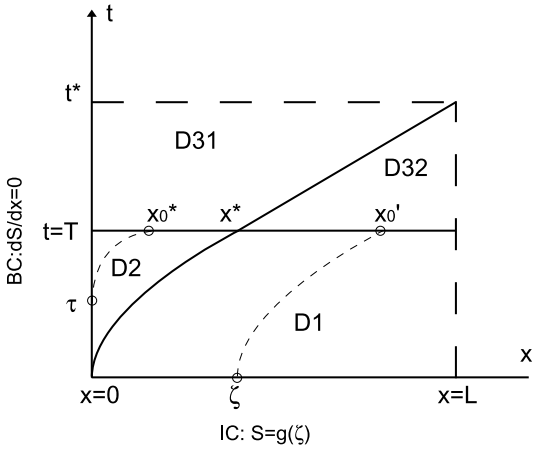

Fig. 4. (x,t) plane with characteristic curves and domain definition.

events with constant intensity and duration T, it is reasonable to assume that the subsurface flow does not reach equilibrium at $t = T$; therefore, four domains can be distinguished (partial equilibrium, see also Fig. 4; the characteristic curve passing through the origin does not reach $x = L$ before $t = T$). Domain 1 (D1) is defined by the characteristic curve $t = t(x,0)$ and the lines $t = 0$ (initial condition), $t = T$ (end of rainfall event), and $x = L$ (outlet of hillslope). To obtain $S(x,t)$ in D1 we solve (8) and (9) subject to the following initial and boundary conditions:

$$t(\zeta) = 0 \quad 0 \leqslant \zeta \leqslant L,$$

$$S(\zeta) = g(\zeta) \quad 0 \leqslant \zeta \leqslant L,$$

where ζ is a parameter representing the intersection of a characteristic curve with the x-axis. The solution in domain D1 is then given by:

$$t = \frac{fL^2}{(2-n)nkH}\left[(1-\zeta/L)^{2-n} - (1-x/L)^{2-n}\right], \tag{10}$$

$$S(x,t) = g(\zeta)\left[\frac{(1-\zeta/L)}{(1-x/L)}\right]^{n-1} + \frac{fL}{nkH}(1-x/L)^{1-n}N[A(x) - A(\zeta)], \tag{11}$$

where $A(x)$ is the upstream drainage area at location x (integral from 0 to x of $w(x)$). For partial equilibrium, domain 2 (D2) is bounded by the characteristic curve $t = t(x,0)$ and the lines $x = 0$ (boundary condition), and $t = T$. The following initial and boundary conditions apply:

$$t(0) = \tau, \quad 0 \leqslant \tau \leqslant T,$$

$$\frac{dS}{dx} = 0, \quad S(0,t) = g(0),$$

where τ is a parameter representing the intersection of a characteristic curve with the t-axis. The solution is now given by:

$$t = \tau - \frac{fL^2}{(2-n)nkH}\left[(1-x/L)^{2-n} - 1\right], \tag{12}$$

$$S(x,t) = -\frac{fL}{nkH}(1-x/L)^{1-n}N\left[\frac{L}{n-1}w(0) - A(x)\right]. \tag{13}$$

When N is considered to be a constant recharge during steady-state subsurface flow, (13) represents the steady-state solution corresponding to this constant recharge rate. Therefore (13) can be used to compute a steady-state initial condition for domain D1, $g(\zeta)$, assuming a given constant recharge rate.

Eqs. (8) and (9) can be simplified for domain D31 and D32 as:

$$\frac{dx}{dt} = -\frac{kz'}{f}, \tag{14}$$

$$\frac{dS}{dx} = -\frac{z''}{z'}S. \tag{15}$$

Domain D31 is defined by the region bounded by the curves $x = 0$, $t = T$, and the characteristic curve passing through x^*. For the definition of the parameter x^* we refer to Fig. 4. The boundary and initial conditions can now be expressed as:

$$t(x_0^*) = T, \quad 0 \leqslant x_0^* < x^*,$$

$$S(x_0^*) = S(x_0^*, T),$$

where x_0^* is a parameter representing the intersection of the characteristic curve through τ and $t = T$. The solution can now be written as:

$$t = T + \frac{fL^2}{(2-n)nkH}\left[(1-x_0^*/L)^{2-n} - (1-x/L)^{2-n}\right], \tag{16}$$

$$S(x,t) = S(x_0^*)\left[\frac{(1-x_0^*/L)}{(1-x/L)}\right]^{n-1}. \tag{17}$$

Domain D32 is defined by the region bounded by the curves $x = L$, $t = T$, and the characteristic curve passing through x^*. The boundary and initial conditions are now given by:

$$t(x_0') = T, \quad x^* \leqslant x_0' < L,$$

$$S(x_0') = S(x_0', \zeta),$$

where x_0' is a parameter representing the intersection of the characteristic curve through ζ and $t = T$. The solution can now be written as:

$$t = T + \frac{fL^2}{(2-n)nkH}\left[(1-x_0'/L)^{2-n} - (1-x/L)^{2-n}\right], \tag{18}$$

$$S(x,t) = S(x_0')\left[\frac{(1-x_0'/L)}{(1-x/L)}\right]^{n-1}. \tag{19}$$

The parameters x_0' and ζ in the above equations are further subject to the following condition:

$$T = \frac{fL^2}{(2-n)nkH}\left[(1-\zeta/L)^{2-n} - (1-x_0'/L)^{2-n}\right]. \quad (20)$$

An important parameter in this solution is x^*. The value of x^* is found through

$$x^* = L\left[1 - \left(1 - \frac{(2-n)nkHT}{fL^2}\right)^{1/(2-n)}\right].$$

2.3. Analytical solutions using (6)

Fan and Bras [2] derived analytical solutions for (5) using (6). Their analytical solutions form a special case to the solutions given here, for the case when $n = 2$. One can derive their Eq. (12) by taking the limit value of (10) and (11) for n approaching 2. Their Eq. (13) however was printed in error (Fan, 2000, personal communications) and should read

$$S(x,0) = \frac{N\left[A(x) + \frac{\beta w(0)}{2\gamma}\right]}{-(k/f)(\beta + 2\gamma x)}. \quad (21)$$

It is important to note at this point that the applied boundary condition ($(\mathrm{d}S/\mathrm{d}x) = 0$) does not guarantee a Dirichlet condition, resulting in the term containing $w(0)$ in (13) as well as (21). In order to prevent mass balance errors for the hillslope, two solutions can be adopted: (i) to assume that $w(0) = 0$, and (ii) to apply a Dirichlet condition ($S(0,t) = 0$ for all t). Both solutions give the same results, viz. the disappearance of the terms containing $w(0)$. The second option, however, is preferred because it does not cause incompatibilities with the assumed plan shape of the hillslope at the divide. Therefore, in the results presented in Section 3.2, the second solution was adopted.

3. Characteristic drainage response functions of basic hillslope types

3.1. Nine hillslope types

One can always approximate a certain portion of the topographic surface of a catchment by a continuous function. An example of such a function is the bivariate quadratic function that was suggested by Evans [28]:

$$z = ax^2 + by^2 + cxy + dx + ey + f, \quad (22)$$

where z is the elevation, x the horizontal distance in the length direction of the area, y the horizontal distance in the direction perpendicular to the length direction (the width direction). The other parameters in the equation are constants. (22) is the general equation of the conic shape. Contour lines on surfaces described by (22) form conic sections. Following [28], we can now characterize hillslopes by the combined curvature in the gradient direction (profile curvature) and the direction perpendicular to the gradient (plan curvature). The profile curvature is important because it reflects the change in slope angle and thus controls the change of velocity of mass flowing down along the slope curve. The plan curvature reflects the change in aspect angle and influences the divergence or convergence of water flow. In other words, profile and plan convexity separate curvature out into two orthogonal components where the effects of gravitational process are either maximized (profile convexity) or minimized (plan convexity). Note that plan curvature is usually measured in the horizontal plane as the curvature of contours, hence its name 'plan curvature' [29,30].

In Section 2, we used a polynomial function to describe the elevation as function of the distance from the slope top (Eq. (7)). Adding a quadratic term to this equation to describe the slope shape in the width direction yields a specific form of the bivariate quadratic function, given by (22)

$$z(x) = E + H(1 - x/L)^n + \omega y^2, \quad (23)$$

where ω is a plan curvature parameter and y is the distance from the slope centre.

Allowing profile curvature (defined by n) to assume values less than, equal to, or greater than 1 and plan curvature (defined by ω) to assume either positive, zero or negative values, one can define nine basic geometric relief forms [31]. Fig. 5 illustrates nine basic hillslope types that are formed by combining three plan and three profile curvatures. In this study we focus on the *shape* of a hillslope in the length direction, while considering the *distance* (not shape) in the width direction. However, the distance in the width direction is a direct consequence of both profile and plan curvature, since these determine

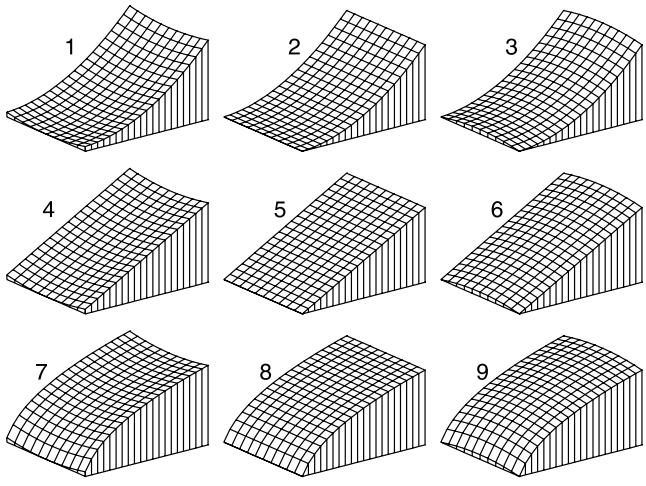

Fig. 5. Three-dimensional view of the nine different hillslopes used in this study. The numbers in the figure refer to Table 1.

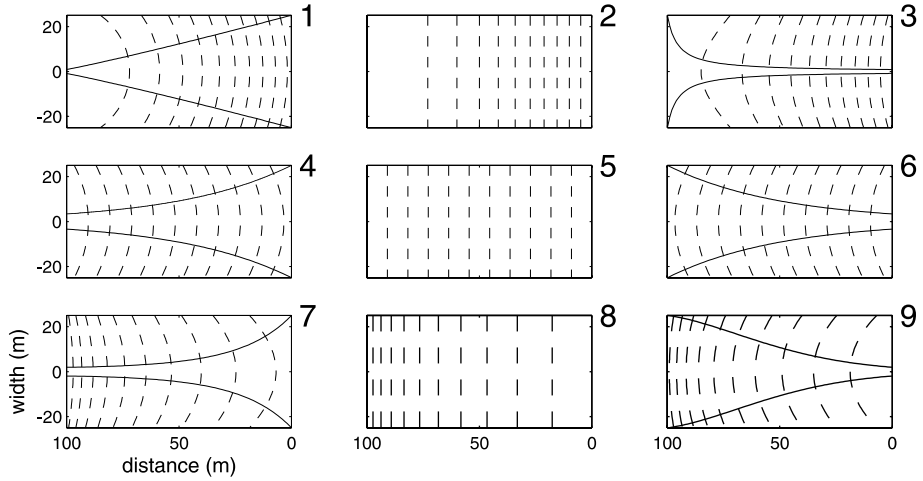

Fig. 6. Plan view of drainage divides (solid lines) and contour lines (dashed lines) of nine hillslopes. The upslope divide of each hillslope is at $x = 0$.

the location of the slope divides. The location of the slope divides as well as some contours are shown in Fig. 6.

The parameters for Eq. (23) are different for each of the nine hillslopes, and listed in Table 1. In particular, the parameter n defines the curvature in the profile direction while ω defines whether the hillslope will converge or diverge. The horizonal length of the nine slopes is chosen to be constant ($L = 100$ m).

These nine hillslopes represent a wide range of hillslope types traditionally considered in hydrology and geomorphology. For different hillslopes within a catchment each individual hillslope type can be fitted using the geometrical scaling parameters H, L, and n to the observed terrain profile curvature, given known soil depth function, and a proper choice of ω to represent the observed $w(x)$. In case the soil depth function is unknown, the profile curvature of the terrain can be assumed to be parallel to the bedrock, thereby assuming constant soil depth function. The soil hydraulic parameters k and f can be obtained by means of hydrograph recession analysis in the case when discharge data are available [32], or be given characteristic values for the soil types present in the catchment.

3.2. Drainage response functions

It is interesting to compare the drainage response functions for these nine hillslopes, as these will reflect the topographic control on the subsurface flow processes. We have therefore conducted the following experiments. Based on the analytical solutions presented in Section 2, we can compute $S(x,t)$ and $Q(L,t)$ using the geometrical parameters listed in Table 1. The soil depth is assumed to be constant ($d = 2$ m). The initial condition is $g(\zeta,0) = \lambda S_c(\zeta)$, where λ assumes a value of 0.2 (20% of maximum storage capacity). The hydraulic parameters are set to $k = 1$ m/h and $f = 0.3$. First, we assume $N = 0$, such that the resulting solution corresponds to free drainage after initial partial saturation.

Figs. 7 and 8 summarize the main results from this experiment. Fig. 7 shows the flow rates, normalized with respect to drainage area, as a function of time and po-

Table 1
Parameters for the nine slopes used in this study

nr	Profile	Plan	H (m)	n (dimensionless)	$\omega \times 10^{-4}$ (m^{-1})	Area (m^2)
1	Concave	Concave	5.01	2	5	2496
2	Concave	Straight	5.01	2	0	5000
3	Concave	Convex	5.01	2	−5	646
4	Straight	Concave	5.25	1	5	2160
5	Straight	Straight	5.25	1	0	5000
6	Straight	Convex	5.25	1	−5	2161
7	Convex	Concave	8.16	0.31	5	1410
8	Convex	Straight	8.16	0.31	0	5000
9	Convex	Convex	8.16	0.31	−5	2386

The last column gives the area of the slope, i.e., the area between the divides shown in Fig. 6. Note that the numbers in the left column correspond with the numbers in Figs. 5–13.

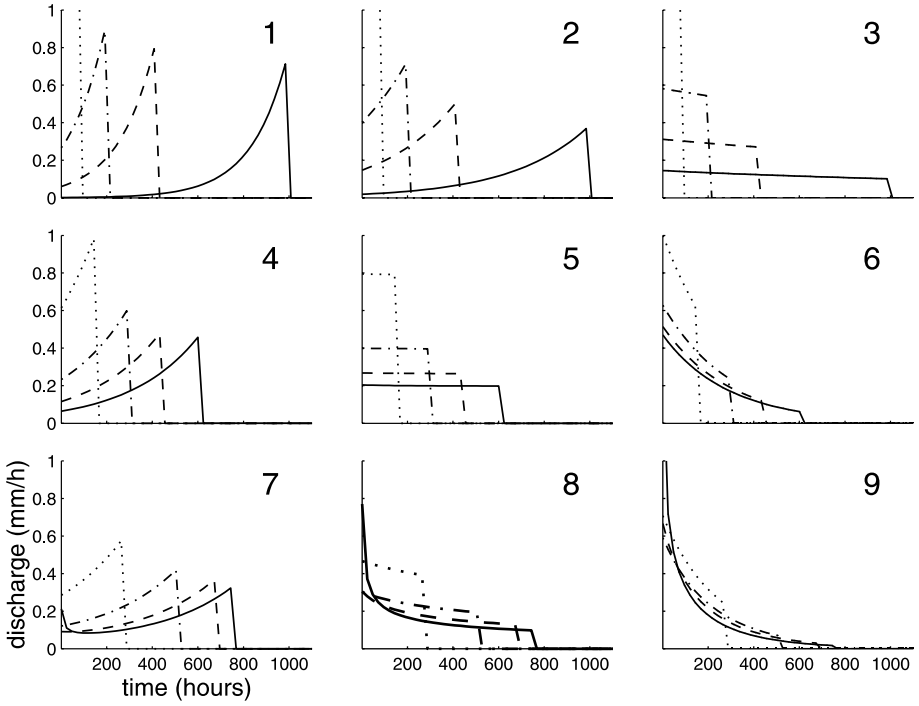

Fig. 7. Normalized subsurface flow rates at different locations along the nine hillslopes during free drainage (dotted line: $x = 25$ m; dash-dotted line: $x = 50$ m; dashed line: $x = 75$ m; solid line: at outlet, $x = 100$ m).

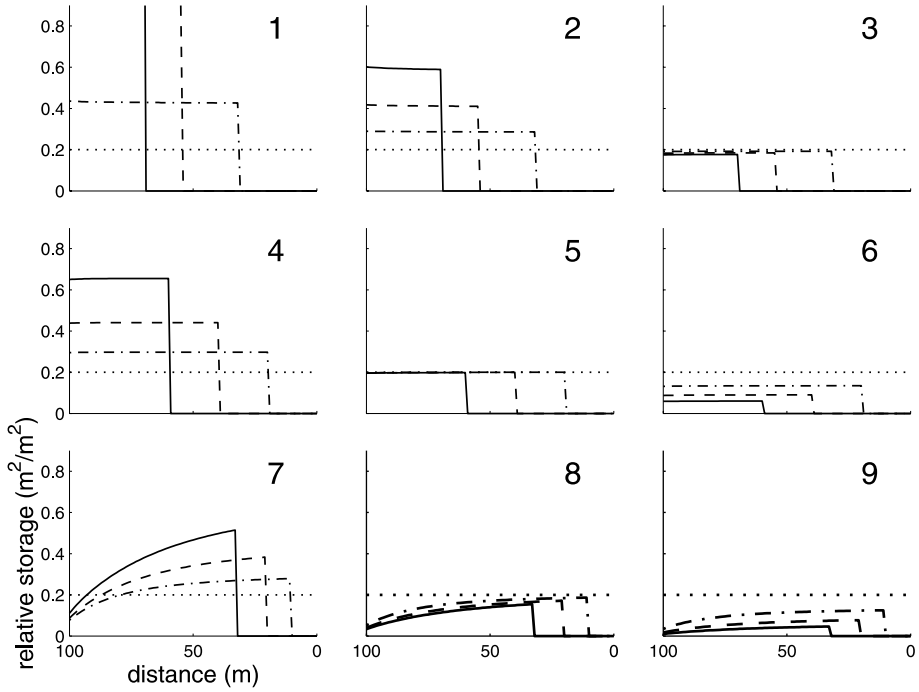

Fig. 8. Relative soil moisture storage for characteristic time steps during free drainage (dotted line: initial time, $t = 0$; dash-dotted line: $t = 5$ days; dashed line: $t = 10$ days; solid line: $t = 15$ days).

sition along the different hillslopes and Fig. 8 gives the evolution of the relative storage function at characteristic time instances. Relative soil moisture storage is defined as the ratio between actual storage, $S(x,t)$, and maximum storage capacity, $S_c(x)$. It is clear that the nine hillslopes show very distinct hydrologic behaviour. Due to the relatively low bedrock slope near the exit, hillslopes 1, 2, and 3 are slowly draining. The outflow for

hillslopes 1, 2, and 4 increases with time due to the increasing soil moisture storage near the exit. The outflow of hillslope 3 stays nearly constant for a long time as the soil moisture storage at the outlet stays close to its initial value before dropping. All convergent slopes (1, 4, and 7) have increasing outflow with time, again because the soil moisture storage at the outlet increases in time. The outflow of 7 initially decreases as the high bedrock slope near the exit allows the storage to drop quickly, but after some time the convergent plan shape causes a build up of storage resulting in an increase of outflow. As expected, the outflow of hillslope 5 stays constant and the initial storage function glides down the slope as a step function. The soil moisture storage near the outlet for the diverging hillslopes (3, 6, and 9) decreases with time. The speed at which this drop in storage occurs depends both on the plan and profile curvature. The combined effect of gradual divergence and convex profile curvature of hillslope 9 results in a fast decrease of storage near the outlet and a corresponding drop of outflow rate. Because of the set-up of this experiment (free drainage and initial uniform partial saturation) we can regard these results as the impulse response functions of the nine hillslopes. As discussed in [18], these impulse response functions can now be used to construct the instantaneous unit hydrograph of subsurface storm flow of a catchment.

A second experiment evaluates the drainage response functions under a constant rainfall recharge event. At time $t = 0$ a rainfall recharge event with intensity $N = 10$ mm/day starts and lasts for the whole duration of the computations, until a steady-state is reached. This value is chosen as it corresponds with typical design storm characteristics used for agricultural drainage purposes. In humid temperate climate conditions such as Northwestern Europe this rainfall event has a return period of about 1 year. Further we assume initially dry conditions ($\lambda = 0$). The results of this experiment are given in Figs. 9 and 10. As expected, hillslope 5 shows the typical ramp response function for subsurface flow rates at different locations along the hillslope. Surprisingly, also hillslope 3 shows such a behaviour. It appears that the decrease in bedrock slope is compensated by the increase in hillslope width. The other diverging hillslopes (6 and 9) as well as hillslope 8 have approximately a first-order step response function for subsurface drainage. The other hillslopes show exponential growth in subsurface drainage until the steady-state condition is reached. Also the corresponding relative storage functions for the different hillslopes are interesting to analyse (Fig. 10). For the rainfall recharge event chosen, only hillslopes 1, 2, and 4 will saturate near the outlet. In the figure we have indicated by arrows the extent of the saturated zone at steady-state. Note that saturation is defined here whenever $S(x,t) \geqslant S_c(x)$ (value 1 on the y axis of Fig. 10). Hillslope 1 has a steady-state saturation of 30%, 14% for hillslope 2, and 11% for hillslope 4. Note that in the case of saturation, the computation of the outflow

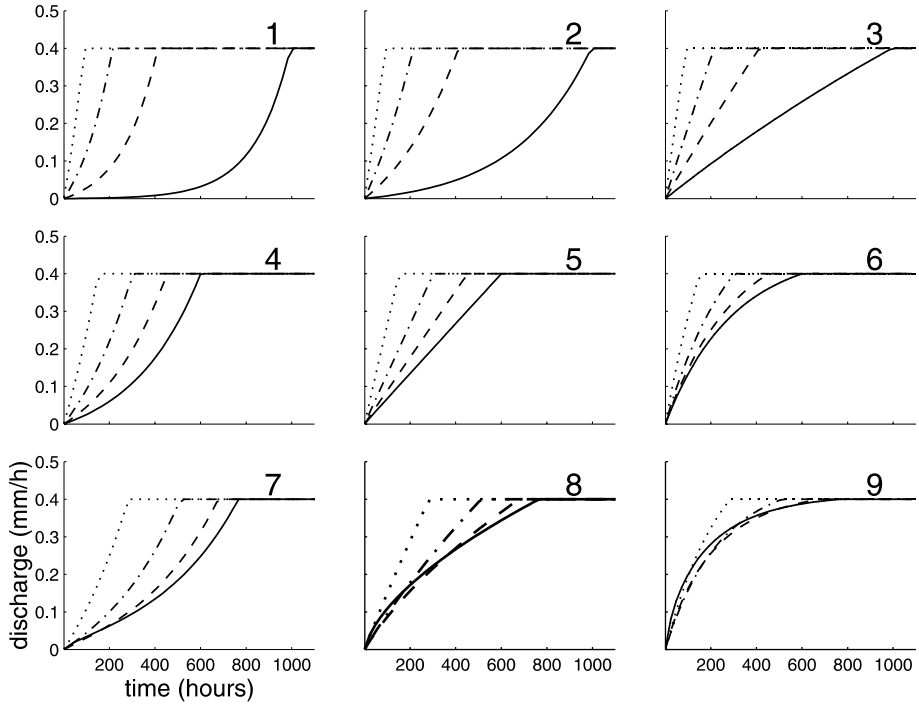

Fig. 9. Normalized subsurface flow rates at different locations along the nine hillslopes during a constant rainfall recharge event, $N = 10$ mm/day (dotted line: $x = 25$ m; dash-dotted line: $x = 50$ m; dashed line: $x = 75$ m; solid line: at outlet, $x = 100$ m).

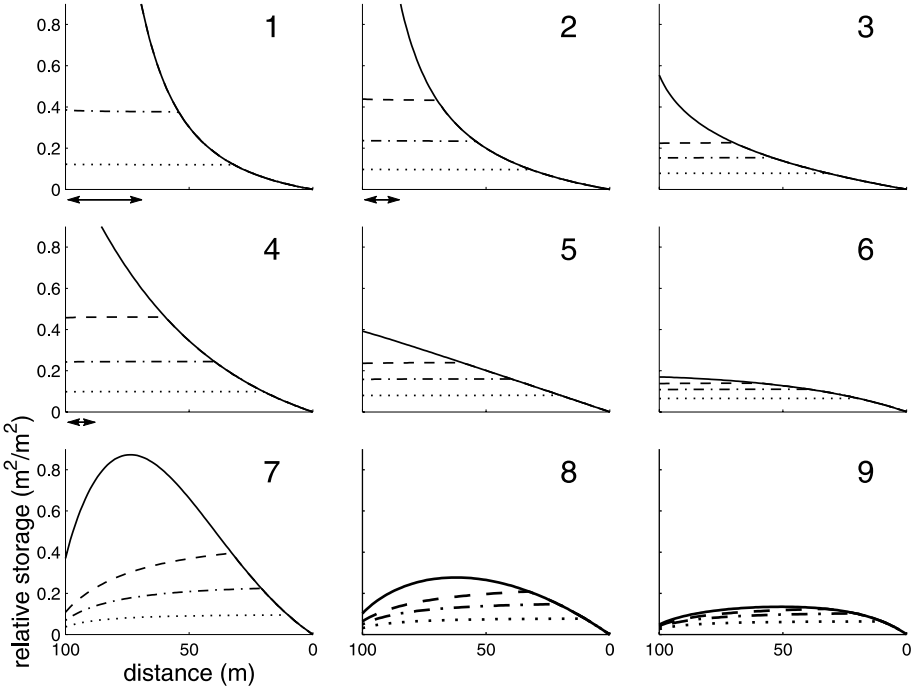

Fig. 10. Relative soil moisture storage for characteristic time steps during a constant rainfall recharge event, $N = 10$ mm/day (dotted line: $t = 5$ days; dash-dotted line: $t = 10$ days; dashed line: $t = 15$ days; solid line: steady-state). The arrows beneath plots 1, 2 and 4 indicate the saturated area of the respective slopes at steady-state.

rate has to be modified to account for return flow. An obvious choice for this overland flow routing problem is the use of kinematic wave routing [2].

3.3. Dimensional analysis

The results presented in Section 3.2 represent the characteristic response functions for a specific set of hillslopes with given hydraulic and geometric properties. In order to illustrate the general character of these response functions we have executed the following dimensional analysis. By defining dimensionless variables we are able to plot the results of our model for a wide range of hillslopes with varying length, maximum storage capacity, average slope angle, and hydraulic conductivity. Moreover, the recharge response under different steady-state rainfall intensities can be included in these plots. We therefore define the following dimensionless variables:

$$\tau = \frac{tki}{L},$$

$$\chi = \frac{x}{L},$$

$$\phi = \frac{Q}{NA},$$

$$\sigma = \frac{Sk}{S_c N}.$$

The variable τ defines the kinematic time [33], where i is average bedrock slope angle χ defines the dimensionless flow distance, whereas ϕ and σ are our new flow variables. Note that the definition of ϕ and σ needs to be modified slightly under free drainage (zero recharge N): in that case the relative flow variable is computed as the ratio between cumulative outflow and initial storage volume and the relative storage variable is defined as the ratio between actual storage and maximum storage capacity. Fig. 11 plots dimensionless outflow, corresponding with $N = 0$, 5, 10 and 20 mm/day, against kinematic time where $k = 0.5$, 1 and 2 m/h. As we can see, all lines collapse to one, which represents the characteristic response function for outflow for the nine distinct hillslopes under study. These functions do not differ from the case study presented in Section 3.2 (Fig. 9), which illustrates once again the general character of the response functions derived from our analytical solutions. Figs. 12 and 13 show the dimensionless storage as function of dimensionless flow distance for the case of free drainage ($N = 0$ mm/day, Fig. 12) and constant recharge ($N = 5$, 10 and 20 mm/day, Fig. 13). Again, exactly the same shape of the storage functions shown in Figs. 8 and 10 appear. It is noteworthy that in order for the curves to overlap we have plotted the corresponding dimensionless storage functions at characteristic kinematic time steps (5, 10, 15 and 30).

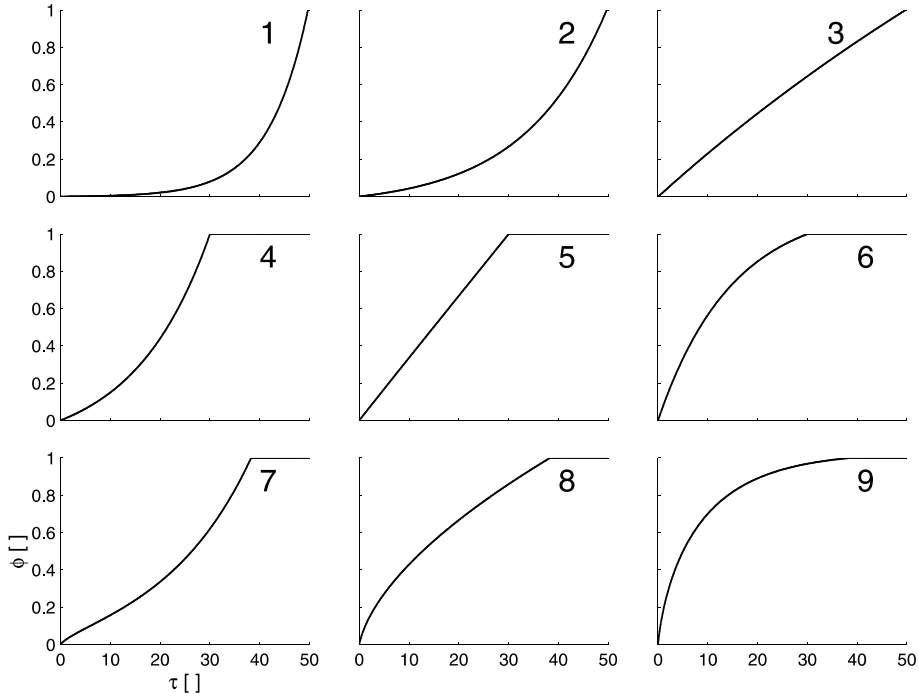

Fig. 11. Dimensionless outflow (ϕ) versus kinematic time (τ) for the nine hillslope types for different hydraulic conductivities ($k = 0.5$, 1, 2 m/h) and different rainfall recharge rates ($N = 0$, 5, 10 and 20 mm/day) – 12 combinations in total. Note that when $N = 0$ mm/day the plotted cumulative outflow is normalized by initial storage volume. The graphs for the 12 different rainfall recharge rates and hydraulic conductivities lay on top of each other.

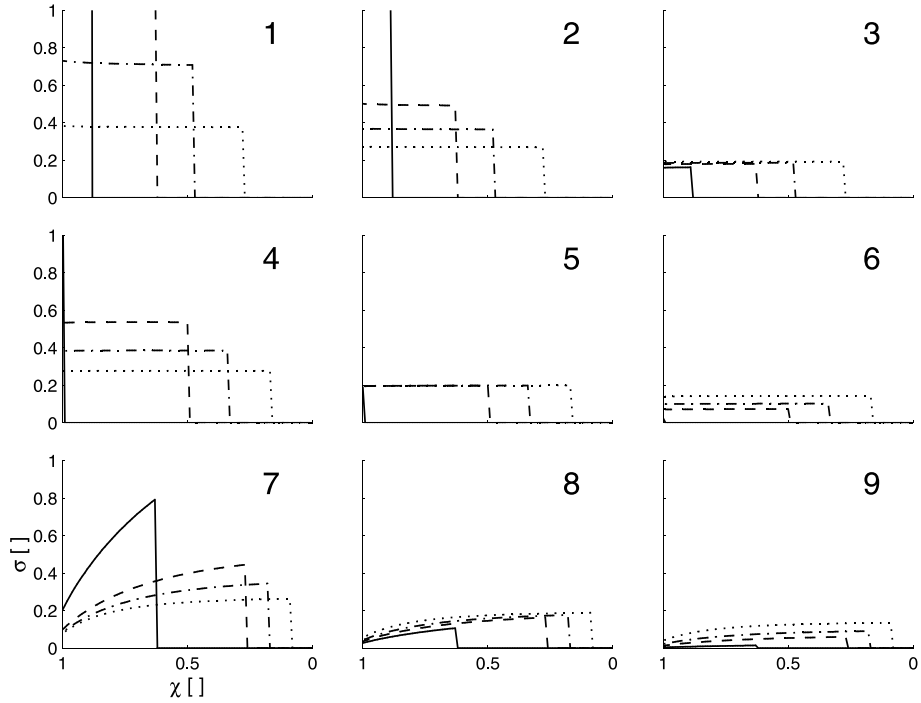

Fig. 12. Dimensionless storage (σ) versus dimensionless flow distance (χ) at kinematic time steps for $k = 0.5$, 1 and 2 m/h and free drainage. The graphs for the three different hydraulic conductivities lay on top of each other. The different lines show the change of dimensionless storage over kinematic time (dotted line: $\tau = 5$; dash-dotted line: $\tau = 10$; dashed line: $\tau = 15$; solid line: $\tau = 30$).

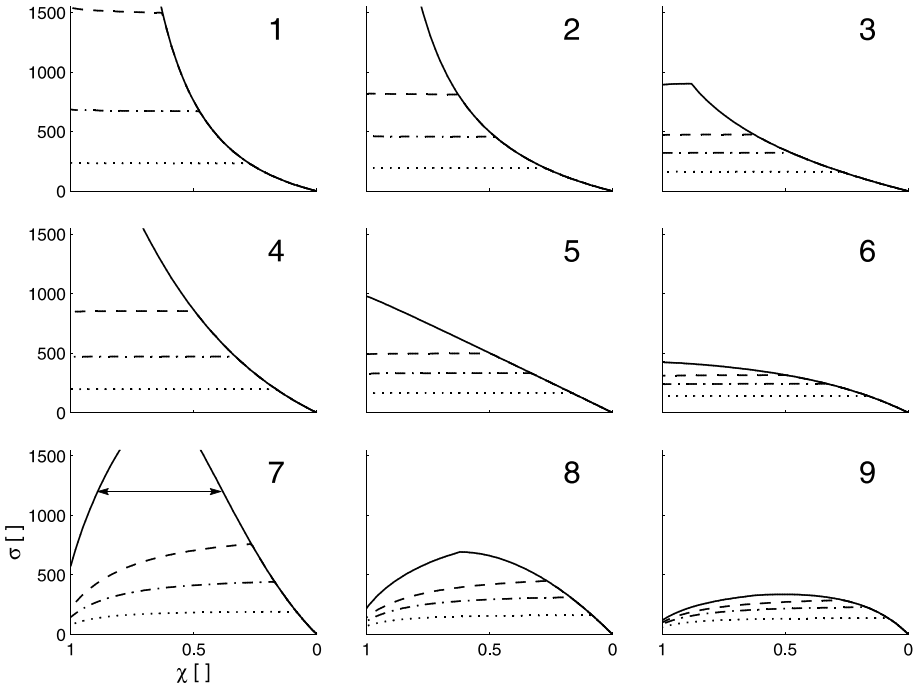

Fig. 13. Dimensionless storage (σ) versus dimensionless flow distance (χ) at kinematic time steps for $k = 0.5$, 1 and 2 m/h and $N = 0$, 5, 10 and 20 mm/day – nine combinations in total. The graphs for the nine different hydraulic conductivities and rainfall recharge rates lay on top of each other. The different lines show the change of dimensionless storage over kinematic time (dotted line: $\tau = 5$; dash-dotted line: $\tau = 10$; dashed line: $\tau = 15$; solid line: $\tau = 30$). The arrow indicates the location of a saturated area for the case where $k = 0.5$ mm/h and $N = 20$ mm/day ($\sigma = 1200$ for $S/S_C \equiv 1$).

4. Summary and concluding remarks

In this paper, we have focused on the study of spatio-temporal dynamics of flow processes in situations where topographic relief and shallow subsurface moisture control the storage and timing of runoff on the landscape. We have started our analysis from the observation that the geometry (that is shape and curvature) of the hillslope exerts a major control on the hydrologic storage-response, by defining the domain and boundary conditions of moisture storage [26]. The equation that describes flow processes in such situations, known as the three-dimensional Richards equation, is highly complex and requires the solution of extremely large systems of equations even for small problems [27]. To overcome this problem an attempt to incorporate the topographic structure of hydrologic processes into the model formulation has been presented. Our approach builds upon the new approach to subsurface flow modeling along hillslopes introduced by [2]. We have presented more general analytical solutions to the hillslope-storage kinematic wave equation for subsurface flow that allow the computation of characteristic response functions for different types of hillslopes. The hillslope-storage subsurface flow equation takes into account the topographic controls exerted on the flow processes by the plan shape and profile curvature. The model has been applied to nine distinct hillslope types which can be viewed as a first-order approximation of the landscape that constitutes a catchment. We have demonstrated that these nine hillslopes show quite different dynamic behaviour during free drainage and rainfall recharge events. In an attempt to facilitate the interpretation of the characteritic response functions we have produced dimensionless plots. We show that the response functions derived from our analytical solutions are indeed characteristic for a given hillslope type. One could also try to capture the three-dimensional shape of hillslopes into a dimensionless representation. This would inevitably lead to the collapsing of the nine subplots in Figs. 7–13 into one, representing the straight constant bedrock sloping hillslope. The authors are currently focussing their research on this idea.

The limitations of our approach are: (1) the kinematic wave assumption of subsurface flow, (2) the assumption of spatially homogeneous hydraulic characteristics of the hillslopes, (3) the assumption that capillarity effects in the unsaturated zone above the phreatic layer can be neglected, and (4) recharge is spatially uniform.

Because we assume that the kinematic wave approximation holds, the solutions presented here are limited to moderate to steep slopes. The lower limit of relevant slopes is defined by the ratio of gravity drainage versus diffusion drainage [12]. Since we have formulated the kinematic form of Darcy's law under the assumption of horizontal flow lines, there exists also an upper limit to

the relevant bedrock slopes [7]. To overcome the limitations of the kinematic wave assumption, our model can be formulated starting from Boussinesq's equation. The formulation of a hillslope-storage Boussinesq equation and its solutions form the focus of a subsequent paper [34].

Beven [35] summarized results from a number of field studies on the variation of saturated hydraulic conductivity and effective porosity with depth below the surface. He used exponential decay functions to describe these dependencies. Robinson and Sivapalan [14] used this relationship to derive analytical solutions to kinematic wave subsurface flow along one-dimensional hillslopes. A similar procedure could be adopted in our model formulation, rendering the resulting solutions more general.

Parlange and Brutsaert [36] extended the linearized Boussinesq equation for a horizontal aquifer by introducing a simple correction term to take capillarity effects on subsurface flow into account. They demonstrated that the required correction can be quite significant for relatively short times. In situations where capillarity effects need to be taken into account a similar procedure could be adopted in our model formulation. The authors are currently investigating the effects of a gradual and diffuse transition zone of partly saturated material by comparing the hillslope-storage equation with numerical simulations based on the three-dimensional Richards equation.

The model developed here assumes spatially uniform recharge. This assumption can only be relaxed if the dynamic equations are solved numerically, since no general analytical solution for spatially heterogeneous recharge is possible. Woods et al. [37] give an excellent discussion on the effect of macropores and preferential flow paths on the generation of subsurface flow and saturation excess runoff. In their paper they recognize that the portion of the rainfall that becomes subsurface runoff will depend on soil characteristics and soil moisture deficit, and both of these features may vary markedly over short distances. However, as also noted by Woods et al. [37], in an environment where subsurface runoff dominates, it is possible that the observable topographic features will control the crucial soil moisture deficits. This renders the approach advocated here of value to capture the main dynamics of subsurface flow along complex hillslopes.

References

[1] Boussinesq J. Essai sur la theorie des eaux courantes. Mem Acad Sci Inst Fr 1877;23(1):252–60.
[2] Fan Y, Bras RL. Analytical solutions to hillslope subsurface storm flow and saturation overland flow. Water Resour Res 1998;34(4):921–7.
[3] Stefano CD, Ferro V, Porto P, Tusa G. Slope curvature influence on soil erosion and deposition processes. Water Resour Res 2000;36(2):607–17.
[4] Rodriguez-Iturbe I, Valdes JB. The geomorphologic structure of hydrologic response. Water Resour Res 1979;15(6):1409–20.
[5] Gupta VK, Waymire E. On the formulation of an analytical approach to hydrologic response and similarity at the basin scale. J Hydrol 1983;65(1–3):463–76.
[6] Mesa OJ, Mifflin ER. On the relative role of hillslope and network geometry in hydrologic response. In: Gupta VK, Rodriguez-Iturbe I, Wood EF, editors. Scale problems in hydrology. Dordrecht: Reidel Publishing Company; 1986. p. 1–17.
[7] Childs EC. Drainage of groundwater resting on a sloping bed. Water Resour Res 1971;7(5):1256–63.
[8] Bear J. Dynamics of fluids in porous media. Mineola, NY: Dover; 1972.
[9] Boussinesq J. Recherches theoriques sur l'ecoulement des nappes d'eau infiltrees dans le sol. J Math Pures Appl 5me Ser 1904;10:5–78.
[10] Polubarinova-Kochina PY-A. Theory of groundwater movement. Princeton, NJ: Princeton University Press; 1962 [Translated from Russian by R.J.M. De Wiest].
[11] Henderson FM, Wooding RA. Overland flow and groundwater flow from a steady rainfall of finite duration. J Geophys Res 1964;69(8):1531–40.
[12] Beven K. Kinematic subsurface stormflow. Water Resour Res 1981;17(5):1419–24.
[13] Germann PF, Pierce RS, Beven K. Kinematic wave approximation to the initiation of subsurface storm flow in a sloping forest soil. Adv Water Resour 1986;9:70–6.
[14] Robinson JS, Sivapalan M. Instantaneous response functions of overland flow and subsurface stormflow for catchment models. Hydrol Processes 1996;10:845–62.
[15] Beldring S, Gottschalk L, Rodhe A, Tallaksen LM. Kinematic wave approximations to hillslope hydrological processes in tills. Hydrol Processes 2000;14:727–45.
[16] Sanford WE, Parlange JY, Steenhuis TS. Hillslope drainage with sudden drawdown: closed form solution and laboratory experiments. Water Resour Res 1993;29(7):2313–21.
[17] Su N. A formula for computation of time-varying recharge of groundwater. J Hydrol 1994;160:123–35.
[18] Brutsaert W. The unit reponse of groundwater outflow from a hillslope. Water Resour Res 1994;30(10):2759–63.
[19] Verhoest NEC, Troch PA. Some analytical solutions of the linearized Boussinesq equation with recharge for a sloping aquifer. Water Resour Res 2000;36(3):793–800.
[20] Sloan WT. A physics-based function for modeling transient groundwater discharge at the watershed scale. Water Resour Res 2000;36(1):225–41.
[21] Betson RP, Marius JB. Source area of storm runoff. Water Resour Res 1969;5(3):574–82.
[22] Dunne T, Black RD. Partial area contributions to storm runoff in a small new England watershed. Water Resour Res 1970;6:1296–311.
[23] Anderson MG, Burt TP. The role of topography in controlling throughflow generation. Earth Surf Processes 1978;3:331–44.
[24] Freeze RA. Three-dimensional, transient saturated–unsaturated flow in a groundwater basin. Water Resour Res 1971;7(2):347–66.
[25] Smith RE, Hebbert RHB. Mathematical simulation of interdependent surface and subsurface hydrologic processes. Water Resour Res 1983;19(4):987–1101.
[26] Duffy CJ, Lee D-H, Jin M-H. Dynamics of soil moisture, subsurface flow and runoff in complex terrain, Tech. Rep. ER9408, Environmental Resour. Res. Institute, PennState, 1994.
[27] Paniconi C, Wood EF. A detailed model for simulation of catchment scale subsurface hydrologic processes. Water Resour Res 1993;29(6):1601–20.

[28] Evans IS. An integrated system of terrain analysis and slope mapping. Z Geomorph NF Suppl-Bd 1980;36:274–95.
[29] Zevenbergen LW, Thorne CR. Quantitative analysis of land surface topography. Earth Surf Processes Landforms 1987;12:47–56.
[30] Moore ID, Grayson RB, Ladson AR. Digital terrain modelling: a review of hydrological geomorphological and biological applications. Hydrol Processes 1991;5:3–30.
[31] Dikau R. The application of a digital relief model to landform analysis in geomorphology. In: Raper J, editor. Three dimensional applications in geographical information systems. London: Taylor and Francis; 1989. p. 51–77.
[32] Troch PA, De Troch FP, Brutsaert W. Effective water table depth to describe initial conditions prior to storm rainfall in humid regions. Water Resour Res 1993;29(2):427–34.
[33] Ogden FL, Watts BA. Saturated area formation on conconvergent hillslope topography with shallow soils: a numerical investigation. Water Resour Res 2000;36(7):1795–804.
[34] Troch PA, Paniconi C, van Loon EE. The hillslope-storage Boussinesq model for subsurface flow and variable source areas along complex hillslopes: 1. formulation and characteristic response. Water Resour. Res. [submitted].
[35] Beven K. On subsurface storm flow: an analysis of response times. Hydrol Sci J 1982;4:505–19.
[36] Parlange J-Y, Brutsaert W. A capillarity correction for free surface flow of groundwater. Water Resour Res 1987;23(5):805–8.
[37] Woods RA, Sivapalan M, Robinson JS. Modeling the spatial variability of subsurface runoff using a topographic index. Water Resour Res 1997;33(5):1061–73.